ChemBioChem

Research Article
doi.org/10.1002/cbic.202200139

Chemistry Europe
European Chemical Societies Publishing

www.chembiochem.org

Trace-Level Phenolics Detection Based on Composite PAN-MWCNTs Nanofibers

Elif Merve Özer,[a] Roxana-Mihaela Apetrei,[a, b] and Pinar Camurlu*[a]

In view of major concerns regarding toxicity (genotoxic, mutagenic, hepatotoxic) of phenolics, there is an on-going necessity for sensitive and accurate analytical procedures for detection and measurements in environmental field, water, and food quality control. The current study proposes composite polyacrylonitrile nanofibrous assemblies enriched with multi-wall carbon nanotubes (PAN-MWCNTs NFs) as suitable immobilization platforms for cross-linking of tyrosinase in detection of both diphenols and monophenols, which are of much interest in water contamination. The prepared biosensor (Pt/PAN-MWCNTs/Tyr) showed high sensitivity in catechol detection (362.5 mA/M.cm^2) and moderate sensitivity for the two monophenols (phenol, *p*-chlorophenol) with 14.79 and 25.46 mA/M.cm^2, respectively. The LOD values of the sensor were in the nanomolar range: 4.42×10^{-9}, 4.06×10^{-7} and 1.05×10^{-7} M for catechol, phenol and *p*-chlorophenol, respectively, allowing detection of trace amounts of phenolics in spiked water samples.

Introduction

Phenolic compounds are essential in biochemical and physiological processes in living organisms, yet their accumulation in the environment has led to widespread contamination from both natural and industrial sources. Since they are used in processes such as production of pesticides, paints, glues, pharmaceutics, textiles etc., phenol contamination of water sources is of particular concern.[1] As such, strict international standards regarding the permissible concentration of phenolics in waters have been instated (maximum limit for phenol in drinking waters is 0.002 mg/L[2]).

The necessity for accurate determination of trace amounts of phenolics has led to the application of classical analytical techniques (chromatography, capillary electrophoresis, chemiluminescence, enzyme-linked immunosorbent assay etc.). However, these methods require complex sample pre-treatment or laborious analysis, thus they are costly and have limited applicability to on-line or field monitoring. Biosensors emerged as a valuable alternative because they can provide rapid response, simplicity in analysis, possibility for miniaturization and portability, and/or multi-component sample analysis *in situ*.[3] In the past five years, over 150 papers devoted to different aspects of electrochemical detection of phenolics have been reported, displaying the considerable scientific significance of the topic.[1]

The basic mechanism of an electrochemical biosensor is based on the proximity between a biorecognition element and a signal transducer. The bio-element recognizes the target molecule, which imparts a chemical change that is transduced into an electrochemical signal.[4] Typically, the biomolecule employed for biorecognition (e.g. enzyme) exhibits high selectivity, allowing specific detection of the desired analyte yet it is extremely sensitive to external environmental conditions, being liable for denaturation and loss of activity. As such, the optimum immobilization of the bio-element plays a crucial role in the analytical performance of the designed biosensor.[5] Not only controlled confinement is required, but there is a need for stable and adequate orientation of the biomolecule to promote efficient mass-transfer and accessibility of the analyte to its active center.[6]

Nanofibrous assemblies are favored as biomolecule immobilization supports due to attractive properties (high surface to volume ratio, low barrier to diffusion and interconnected porosity), which allow a much higher biomolecule loading than other substrates (membranes, films). The improved activity retention is maintained at varying external factors (temperature, pH|) leading to increased operational and storage stability.[7,8] Considering the state of the art in biomolecule immobilization, nanofibers (NFs) represent excellent substrates for high loading, catalytic efficiency, and stability.[9,10] Electrospinning is an excellent technique for generating such NFs in a facile, inexpensive manner than confers a great degree of versatility and control over desired properties (NF mat thickness, surface area to volume ratio, pore size and distribution).[11]

Determination of phenolics has been widely researched and a variety of materials (such as chitosan,[12] cellulose biopolymers,[13] poly(vinyl alcohol)[14] etc.) proved suitable as immobilization matrices in removal or degradation of toxicants. Additionally, conducting nanostructures (quantum dots,[15] carbon nanotubes,[16,17] graphene,[18] nano-diamonds,[19] metallic nanoparticles[20,21] have been incorporated for attaining close contact between the transducer and the immobilized biomolecules to enhance the detection efficiency.[1] In particular, CNTs were highlighted due to high conductivity, mechanical strength

[a] *E. M. Özer, R.-M. Apetrei, P. Camurlu*
Akdeniz University
Department of Chemistry, 07058 Antalya (Turkey)
E-mail: pcamurlu@akdeniz.edu.tr
[b] *R.-M. Apetrei*
Dunarea de Jos' University of Galati
Domneasca Street, 47, Galati 800008 (Romania)

Supporting information for this article is available on the WWW under https://doi.org/10.1002/cbic.202200139

and high surface area, thus promoting efficient electrode transfer between enzyme and electrode[22] and reinforcing the detection platform. The functionalization of the nanocarbon is also significant as it increases the processability and applicability.[23–25]

Thus far, the synergy of this concept was mostly evaluated on film or beads matrices with few recent reports on laccase immobilization on cellulose NFs for dye effluent treatment,[26] poly(vinyl alcohol) and poly(acrylonitrile) NFs for removal of 2,4-dichlorophenol[27] and 2,4,6-tricholorophenol,[28] electrospun zein/zein-polyurethane fibers for bioconversion of phenyl urea herbicide[29] or poly(vinylpyrrolidone)/chitosan NFs for electrochemical detection of 17α-ethinylestradiol.[30]

In this context, the enzymes employed are part of the polyphenol oxidases (PPOs) class. Tyrosinase, Laccase and Catechol oxidase have similar structures (metallic active situs with Cu center(s) coordinated by histidine, cysteine and methionine amino acids) and somewhat overlapping substrates.[31] Tyrosinase (E.C. 1.14.18.1, monophenol monooxygenase) catalyzes two consecutive oxygen-dependent reactions, i.e. the *o*-hydroxylation of monophenols to *o*-diphenols (cresolase activity) and the oxidation of respective *o*-diphenols to *o*-quinones (catecholase activity) with water as by product.[32] The former catalytic mechanism can be considered unique as it is particular to Tyr and not exhibited by enzymatic analogues. Its most significant catalytic reaction is the oxidation of L-tyrosine to L-DOPA, a rate-limiting step in the production of dopamine (involved in Parkinson's disease)[33] and melanin. Hence, the catalytic mechanism and basic structural features of Tyr have been thoroughly investigated.[34]

The current study considered the beneficial effects of nanofibrous assemblies as immobilization supports in biosensing of other analytes (glucose, urea),[35] the recent progress made in laccase immobilization on NFs for bioremediation purposes as well as the influence of conducting nanostructures[36] and introduces a biosensing platform based on composite polyacrylonitrile-carboxyl multi-wall carbon nanotubes NFs (PAN-MWCNTs NFs). PAN is a widely available polymer, with good mechanical strength and high thermal resistance[37] rendering ease in electrospinning of both pristine and composite NFs. The concept is designed to be facile and relatively low cost as it does not involve complex synthesis of expensive nanostructured elements, nor it requires additional reagents for analysis. Tyrosinase was chosen as the phenol-selective biomolecule due to particularities of catalysis, which allow for detection of catechol, but also phenol and substituted phenols, which are of much interest in contamination of water sources. The prepared biosensor (Pt/PAN-MWCNTs/Tyr) was evaluated in the detection of an *o*-diphenol (catechol) and two monophenols (phenol, *p*-chlorophenol) and showed discrepancy in sensitivity according to the phenolic class (mono- vs. diphenol). The LOD values of the sensor were in the nanomolar range with minimal interference, leading to adequate detection of phenolics at trace-level in spiked water samples.

Results and Discussion

Morphological characterization

The morphological characterization of the PAN-MWCNTs NFs was previously discussed when the platform was employed for glucose detection.[38] The nanofibers formed have partially bead defects given by the incorporation of MWCNTs as commonly reported in literature data.[39,40] The optimum concentration of CNTs herein was chosen according to the previous study; however, the supporting polymer concentration was decreased to 7% (rather than 10%) in order to increase the ratio of conducting element within the nanocomposite, decrease the fiber diameter (down to 170 nm) (Figure 1), and, in turn increase the surface area and availability for biomolecule loading.

Analytical characterization

Firstly, the electrochemical behavior of the biosensing platform upon addition of small concentrations of different analytes was investigated by CV (Figure 2) and revealed cathodic current change within the selected potential range. The principle of detection involves enzymatic oxidation of the phenolic compound (e.g. catechol) followed by electrochemical reduction of the electroactive quinone species generated as a result. The increase in reduction peak testifies to the efficiency of electron transfer between the electroactive product of enzymatic catalysis (*o*-quinone) and the composite nanofibrous transducer platform. Moreover, it allows estimation of the optimum potential for chronoamperometric analysis, which, in this study, was evaluated at 0.0 V vs. Ag/AgCl for both mono- and diphenol substrates which is commonly reported for PPO-based sensors.[41,42]

Optimum pH value for immobilized mushroom Tyr activity has been established between 7.0 and 8.0 insodium phosphate buffer[43] and in this case, amperometric calibration studies at increasing pH values revealed extended linear range and increase in sensitivity at pH 8.0 (Figure S1).

The optimized conditions were employed in the chronoamperometric study of the developed biosensor platform with

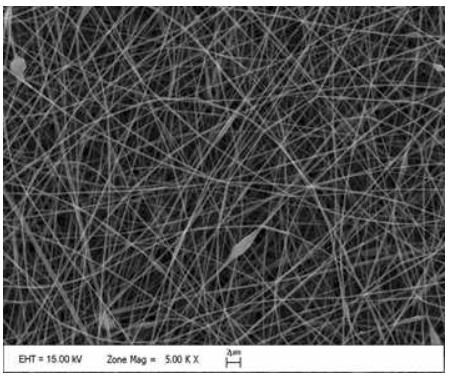

Figure 1. Morphology of PAN-MWCNTs NFs.

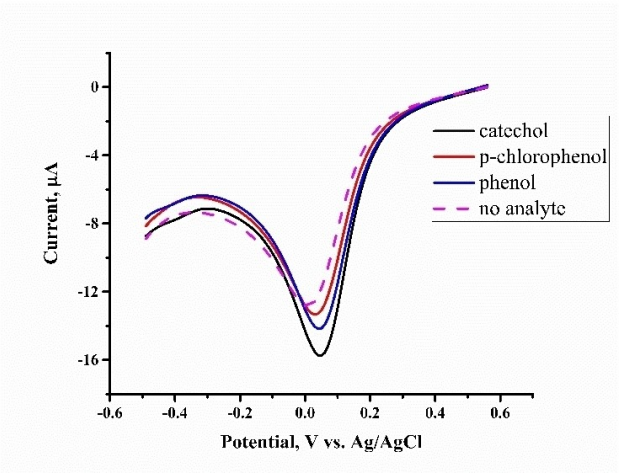

Figure 2. Electrochemical characterization of Pt/PAN-MWCNTs/Tyr biosensor platform before and after addition of catechol (100 μM), phenol and *p*-chlorophenol (0.05 mM) (Sweep rate of 100 mV/s in 0.1 M pH 7.5 PBS).

three phenolic compounds: one *o*-diphenol (catechol) and two monophenols (phenol, *p*-chlorophenol). Progressive additions led to amplification in cathodic current as the concentration of phenolic species to be regenerated at the electrode surface was increased. Figure 3 illustrates the linear current response for catechol in the range 6.00×10^{-8}–1.6×10^{-5} M with a high sensitivity of 362.5 mA/M.cm^2 (y = 7.256x–2.395 (R^2 = 0.995)). The very low LOD value of 4.42×10^{-9} M, calculated according to the slope, proves that the proposed biosensor matrix renders itself useful in ultra-trace detection of catechol.

The calibration curves for detection of monophenols with the Pt/PAN-MWCNT/Tyr biosensor are depicted in Figure 4. Two consecutive linear ranges, up to 2.2×10^{-4} M, were observed with similar sensitivities (in the lower range) of 14.79 (y = 0.295x–5.01 (R^2 = 0.98)) and 25.46 mA/M.cm^2 (y = 0.51x–9.33 (R^2 = 0.98)), for phenol and *p*-chlorophenol, respectively. In accordance, the calculated LOD values were in the higher nanomolar range (4.06×10^{-7} and 1.05×10^{-7} M, respectively).

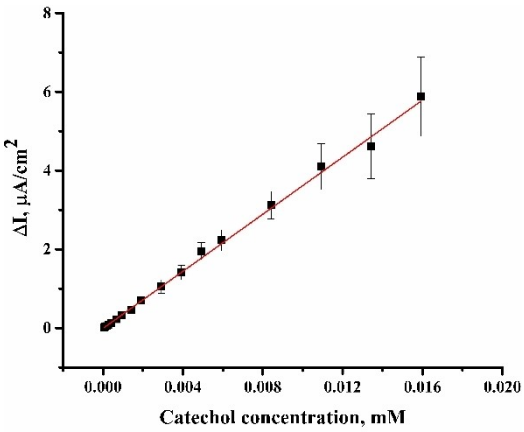

Figure 3. Calibration curve for catechol detection with Pt/PAN-MWCNT/Tyr biosensor (0.0 V vs. Ag/AgCl; 0.1 M PBS pH 8.0, room temperature).

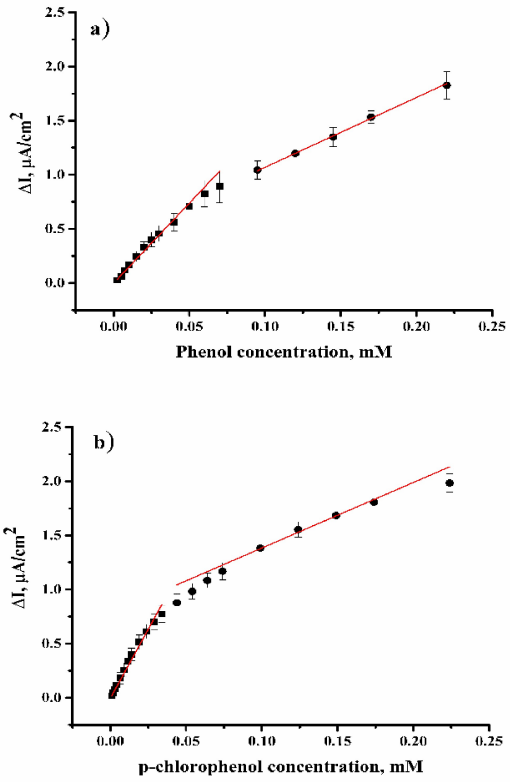

Figure 4. Calibration curve for a) phenol and b) *p*-chlorophenol detection with Pt/PAN-MWCNT/Tyr biosensor (0.0 V vs. Ag/AgCl; 0.1 M PBS pH 8.0, room temperature.

There are a few rate limiting steps involved in phenol biosensing such as (i) diffusion and solubility of substrates, (ii) the rate of electrochemical reduction of *o*-quinone at the electrode surface and (iii) the enzymatic reaction kinetics. In this instance, all biosensors were constructed and evaluated in the same manner whilst the substrate differed, so the latter factor is considered predominantly. It results that such a discrepancy in analytical parameters for detection of mono- vs. diphenols is a result of substrate specificity of the chosen enzyme. This is proven by values calculated for the K_M constant from nonlinear regression of the Michaelis-Menten equation. The lowest K_M value of 0.026 mM was obtained for catechol and an increase up to 0.084 and 0.154 mM was observed for *p*-chlorophenol and phenol, respectively.

Albeit the value of the K_M constant is only apparent since the effect of O_2 concentration (the co-substrate of the enzymatic reaction) was not studied, the data shows a general trend of substrate affinity with catechol as most suitable and phenol, least favorable (catechol > chlorophenol > phenol), which has been observed for some of the Tyr-based biosensors reported.[7,42,44] At this point, the double catalytic action of the enzyme must be considered; the cresolase activity is responsible for hydroxylation of monophenols and the catecholase for conversion of aromatic structures to quinones. The former exhibits a lag period as kinetic studies show for mushroom

tyrosinase because the monophenol hydroxylation requires the enzyme in the 'oxy state' and, typically, only a small portion of the resting enzyme is in this state, the larger portion being in the 'met state'. The latter reaction is more easily achieved because for catecholase catalysis, the polyphenols bind to the Cu center in 'met state'.[45] Steady-state kinetic studies have shown that the catecholase reaction is much faster than the cresolase one and the stoichiometry of the reaction implies that one Tyr molecule must achieve two turnovers in the monophenolase cycle for each one in the diphenolase cycle.[46,47] As such, a higher enzyme concentration would be required to achieve the same sensitivity for phenol as for catechol. In addition, *o*-diphenol (catechol) has been reported as one of the most favorable substrates for mushroom tyrosinase.[45,48] Alternatively, the fast kinetics involving catechol lead to catechol self-inhibition of tyrosinase, so-called 'suicide inactivation'[49] after a certain amount of catechol has been converted to quinone.[50] This is indicated by the narrower linear range for catechol than for the other substrates.

The slight superiority of *p*-chlorophenol over phenol may be due to the position and type of substituent, as substituents in *para*- position have been shown as more favorable substrates for tyrosinase due to the electron-withdrawing character of halide substitution.[51] This was reported when enzymatic assays comparing the affinity of Tyr towards catechol and *p*-chlorocatechol were performed.[52]

Nonetheless, the discrepancy in analytical parameters according to the phenolic class might prove advantageous in practical applications as it can discriminate between different phenolic classes of contaminants when the concentration is known. An amperometric analysis to depict this discrepancy is given in Figure S2 where the same concentration of each analyte is added in continuous system and the response is over tenfold higher for catechol than the monophenols as expected from calibration studies (comparison between the calibration curves given in Figure S3 accompanied by detailed analytical parameters (Table S1)). A second addition of catechol after monophenols additions shows a very similar response to the first one therefore the change in type of phenolic substrate does not appear to lead to any enzymatic inhibition.

Furthermore, a comparison with literature data is illustrated in Table 1 (for catechol substrate) and Tables S2, 3 (for phenol and *p*-chlorophenol). The reported analogues (Table 1) have been published within the last five years, thus representing the 'state-of-the-art' in phenolics detection. The proposed biosensing platform has competitive characteristics with one of the lowest LODs reported, even though some of the published works include more complex matrices consisting of gold nanoparticles, nanocrystalline diamond, magnetite etc. On this note, preparation of an efficient but facile and relatively inexpensive matrix such as the one tested herein may prove more advantageous for development of disposable, portable sensors for on-line or field measurements.

A report on hybrid PVA-silica NF mats proved similar performance but with over 10^3 higher LOD.[53] Thus, the performance of our biosensor is not only the result of the large surface area of the NFs, but also of the reinforcement with COOH-MWCNTs.

Stability and real sample determination

The stability of the proposed biosensors was investigated both in operational and storage conditions (Figure S3). Since catechol was shown as the most suitable analyte whilst also being a factor in enzyme inactivation, the analysis was focused solely on it. Stability is commonly troublesome for Tyr sensors due to few factors: (i) Tyr is inherently a relatively unstable enzyme with short lifetime,[65] (ii) formation of catalytic intermediates (radical origin) that can lead to electrode fouling.[66]

In this study, immobilization of Tyr on composite NFs provided above average stability: ~99% of activity was maintained within six consecutive trials, ~75% was leftover by the 20th measurement with relative standard deviation (RSD) value of 14.17% and the shelf life was maintained for the first 20 storage days with over 85% of initial performance preserved, yet it decreased to 50% by the 35th day.

The end goal of preparing a Tyr biosensor is testing the accuracy in detection of phenolics in real samples. Prior to that, the interference to common substances was tested (Figure 5)

Table 1. Summary of reported Tyr-based catechol biosensors.

Tyr biosensor	Linear range (10^{-4} M)	Sensitivity	LOD (10^{-6} M)	Refs.
SPCE/Gr-Au-Chit	5.0×10^{-4}–11.0×10^{-2}	0.483 μA/μM	2.0×10^{-2}	[56]
GCE/GO/GA	5.0×10^{-4}–0.5	0.34 μA/μM	3.0×10^{-2}	[42]
GCE/AuNPs-DHP	2.5×10^{-2}–0.95	115 mA/M	0.17	[53]
BDND	5×10^{-2}–1.2	95.6 mA/M.cm^2	3.28	[54]
CTAB-NCC/QDs	1×10^{-2}–0.25	0.017 μA/μM	0.125	[59]
TMCG	1×10^{-2}–0.3	0.057 A/M	0.26	[58]
NAC-AuNPs/Chit	1×10^{-3}–0.6	0.583 A/M	5.0×10^{-2}	[7]
ITO-silica-PVA	0.1–2.0	0.0057 μA/μM	10	[55]
Pt/poly(2,7-BSeC)	$1.5\times10^{-}$–0.8	2.45 μA/mM	2.0×10^{-2}	[57]
Pt/PAN-MWCNTs	6.0×10^{-4}–0.16	362.5 mA/M.cm	4.42×10^{-3}	This work

SPCE: screen-printed carbon electrode, Gr: graphene, Au/AuNPs: gold nanoparticles, Chit: chitosan, GCE: glassy carbon electrode, GO: graphene oxide, GA: glutaraldehyde, DHP: dihexadecylphosphate, BDND: boron-doped nanocrystalline diamond, CTAB: cetyltriammonium bromide, NCC: nanocrystalline cellulose, QDs: quantum dots, TMCG: magnetite chitosan nanocomposite, NAC-AuNPs: *N*-acetyl-L-cysteine capped AuNPs, ITO: indium tin-oxide, PVA: poly vinyl alcohol, poly(2,7-BSeC): poly[2,7-bis(selenophene)-*N*-nonylcarbazole]

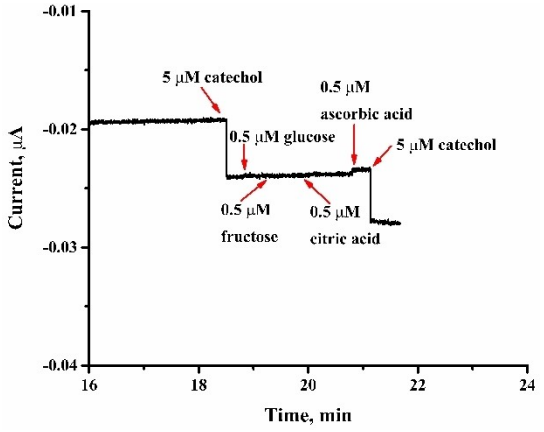

Figure 5. Amperometric response of the Pt/PAN-MWCNT/Tyr biosensor to catechol vs. glucose, fructose, citric and ascorbic acid (0.1 M PBS pH 8.0 at 0.0 V).

showing that sugars (glucose, fructose) or citric acid have no effect on current response. These were chosen as they are common interferents found in phenol-containing foods or beverages and the results reflect the selectivity of the enzymatic catalyst. The only slight change in current was observed upon addition of ascorbic acid. This change consists in decrease of the recorded signal (cathodic peak) while phenol detection in this system leads to increase in cathodic current. This is because the mechanism is based on enzymatic generation of quinone from mono- and diphenols followed by electrochemical reduction of the formed quinone. Increased catechol concentration leads to increased quantity of quinone to be reduced, thus higher cathodic peak. However, oxidation of ascorbic acid at low potentials (in the absence of biorecognition molecule) may occur with associated increase in current and hence the presence of ascorbic acid will be reflected in a decrease of the phenol or catechol current with respect to the current obtained in absence of ascorbic acid (as previously reported).[67] Thus, ascorbic acid, contrary to a typical interferent, that leads to overestimation of analyte in real samples, can have underestimation effect in this case, although the reasoning for it is similarly based on electrocatalytic oxidation.

Moreover, ascorbic acid has the ability to recycle the quinone (generated enzymatically) back to catechol,[68,69] thus directly competing with the electrochemical detection mechanism. However, compared to previous publications, the effect is minor in this study; moreover, the second addition of catechol showed very similar current response to the first, thus, there was no observable inhibition caused by ascorbic or citric acid.

Since the proposed platform can detect both mono- and diphenols and water contamination is one of the prevalent concerns, tap water samples were analyzed. Since they showed no phenol contamination, they were spiked with each of the tested phenolic compounds in varying concentrations. The accuracy of the analysis was calculated, concluding in real sample recovery close to 100% (Table 2) suggesting that the proposed biosensor could be successfully applied in detection of trace phenolic contaminants in water sources.

Table 2. Real sample recovery obtained with the Pt/PAN-MWCNTs/Tyr biosensor (n = 3).

Sample			Added [μM]	Found [μM]	Recovery [%]
Sample 1	–	catechol	0.010	0.00972	97.19
	–	catechol	0.002	0.00203	101.67
Sample 2	–	phenol	0.1000	0.09877	98.77
	–	phenol	0.0025	0.00244	97.66
Sample 3	–	chlorophenol	0.030	0.30179	100.6
	–	chlorophenol	0.003	0.00301	100.43

Conclusion

The current study tested a straightforward approach for phenolics detection based on electrospun PAN NFs reinforced with COOH-MWCNTs as platform for high loading and stable immobilization of Tyr enzyme. The efficacity of the method was proven by the high sensitivity (362.5 mA/M.cm^2) and low LOD (4.42×10^{-9} μM) values obtained in detection of catechol. In addition, phenol and substituted phenol (*p*-chlorophenol) were considered for analysis in view of environmental pollution and water contaminations. The analyses showed LOD values in the nanomolar range. The discrepancy in sensitivity according to the phenolic class (mono-phenols vs. diphenol) is interesting and can be considered a result of specific enzymatic affinity for substrate as different catalytic functions of the enzyme are involved in detection of different phenolic classes. The cresolase activity of Tyr enzyme, responsible for hydroxylation of monophenols (phenol, chlorophenol) requires the enzyme in the 'oxy state' and, typically, only a small portion of the resting enzyme is in this state, the larger portion being in the 'met state'. The catecholase activity leading to conversion of aromatic structures to quinones is more easily achieved because the diphenols (e.g. catechol) bind to the Cu center in 'met' state. The enzymatic mechanism is displayed by the analytical performance of the developed biosensor which proves suitability of the developed NF matrix in preserving native enzyme activity. Due to minimal interference effects, detection of all three phenolic compounds in spiked water samples was performed with high accuracy at trace level, which could be relevant for environmental concerns.

The proposed concept is relatively facile and cost-efficient, does not require synthesis of complex or expensive nanostructures nor the use of additional reagents, thus can render itself to miniaturization for portable sensors in field monitoring.

Experimental Section

Chemicals: Tyrosinase from mushroom (2687 units/mg), polyacrylonitrile (PAN, Mw:150000 g/mol), *N*,*N*-dimethylformamide (DMF, 99%), glutaraldehyde solution (50 wt% in H_2O), sodium dodecyl sulfate (SDS) (ACS reagent, ≥99.0%), D-glucose (99%), sucrose (99%), citric acid (99%), ascorbic acid (99%), 1,2-dihidroxybenzene

(catechol), phenol, *p*-chlorophenol, disodium hydrogen phosphate and sodium dihydrogen phosphate were purchased from Sigma-Aldrich or Merck. (-COOH) functionalized multi-wall carbon nanotubes (>96% purity, 8–18 nm) were purchased from Nanografi Nanotechnology. The ultrapure water (18.2 mΩ/cm was from a direct-Q® Water Purification System (Merck Millipore). All other chemicals were of analytical grade and used without any purification.

Apparatus: Electrochemical analysis and amperometric measurements were performed by Ivium Compactstat. The three-electrode configuration used in all studies includes Ag/AgCl (3 M KCl) as reference electrode, Pt wire as counter electrode and Pt electrode (CH-102, MF-2013) as working electrode. Morphological analysis of the NFs were performed by Zeiss LEO 1430 scanning electron microscope (SEM). The electrospinning assembly used to prepare PAN-CNT nanofibers consists of a DC power supply (GAMMA ES30P, USA), a syringe pump (New Era Pump Systems NE 300, USA) and a collector. The optimum electrospinning parameters were 0.5 mL/h, 15 kV and 25 cm.

Preparation of composite nanofibers: Electrospinning solutions of PAN-MWCNTs were prepared by dissolving predetermined amounts of PAN and MWCNTs separately in DMF and stirred overnight. Subsequently, the MWCNTs solution was added into the PAN solution and then kept in constant stirring for minimum 24 h. The concentration of PAN was kept constant at 7 wt% and the ratio PAN:CNT was 10:1. For morphological characterization, the nanofibers were spun on an aluminum foil and for biosensor construction, a Pt disk electrode was used.

Fabrication of Pt/PAN-CNT/Tyr biosensors and amperometric measurements: After electrospinning on the surface of the Pt disk electrode, enzyme was immobilized by cross-linking. Tyrosinase solution (5 μL in ultrapure water) equivalent to ~134.35 U was dropped onto PAN-CNT nanofibers and left to dry. Subsequently, glutaraldehyde solution (1% w/v in ultrapure water) was dropped on the enzyme-electrospun surface and left to dry at room temperature. The resulting enzyme electrodes were stored at refrigerator conditions in sodium phosphate buffer (PBS; 0.1 M, pH 7) overnight before use.

Amperometric measurements were performed under continuous magnetic stirring monitoring at 0.0 V vs. Ag/AgCl. Increasing concentrations of phenolic content were added in steady-state conditions in the electrolyte (12 mg SDS/10 ml 0.1 M PBS) until the slope between substrate concentration and current response deviated from linearity. The sensitivity was calculated from the slope between current difference (Δ) in μA versus analyte concentration in mM divided by the value calculated as area of the electrode based on the diameter of Pt disk. The calibration plots were obtained by calculating average and standard deviation of the current value for each analyte concentration (n=3). Limit of detection was calculated using 3Sb/m criteria, where m is the slope of the calibration curve and Sb is the standard deviation of the responses at minimal concentration (n=10).[70] The values of I_{max} and the apparent Michaelis-Menten constant (K_M) were calculated based on the nonlinear method[71] (using GraphPad Prism9 software). Interference studies were performed with a ratio of 1:10 interfering compound: catechol. Relative standard deviation (RSD) was calculated as standard deviation /average of all measurements. The applicability of PAN-CNT / Tyr biosensors in real samples, the content of phenolic compounds (catechol, phenol and 4-chlorophenol) in tap water were tested using the spike analysis method.

Acknowledgements

This study was partially supported by Akdeniz University Scientific Research Project Coordination (Project number: FDK-2020-5311).

Conflict of Interest

The authors declare no conflict of interest.

Data Availability Statement

The data that support the findings of this study are available from the corresponding author upon reasonable request.

Keywords: biosensors · carbon nanotubes · electrospun nanofibers · polyacrylonitrile · tyrosinase

[1] P. A. Raymundo-Pereira, T. A. Silva, F. R. Caetano, L. Riboviski, E. Zapp, D. Brondani, M. F. Bergamini, L. H. M. Junior, C. E. Banks, O. N. Oliveira, Jr., *Anal. Chim. Acta* **2020**, *1139*, 198–221.
[2] W. H. Organization, *International Standards for Drinking-Water*, 3rd ed., **1963**.
[3] F. Karim, A. Fakhruddin, *Rev. Environ. Sci. Bio/Technol.* **2012**, *11*, 261–274.
[4] S. P. Mohanty, E. Kougianos, *IEEE Potentials* **2006**, *25*, 35–40.
[5] V. L. Sirisha, A. Jain, A. Jain, *Enzyme Immobilization: An Overview on Methods, Support Material, and Applications of Immobilized Enzymes* (Eds.: S.-K. Kim, F. Toldrá), *Advances in Food and Nutrition Research*, Academic Press **2016**, Ch. 9.
[6] R. M. Apetrei, P. Camurlu, *J. Electrochem. Soc.* **2020**, *167*, 037557.
[7] W. Dong, J. Han, J. Shi, W. Liang, Y. Zhang, C. Dong, *Chin. J. Chem.* **2017**, *35*, 1305–1310.
[8] Z. G. Wang, L. S. Wan, Z. M. Liu, X. J. Huang, Z. K. Xu, *J. Mol. Catal. B* **2009**, *56*, 189–195.
[9] B. Ding, M. Wang, X. Wang, J. Yu, G. Sun, *Mater. Today* **2010**, *13*, 16–27.
[10] S. Smith, K. Goodge, M. Delaney, A. Struzyk, N. Tansey, M. Frey, *Nanomaterials* **2020**, *10*, 2142.
[11] N. Bhardwaj, S. C. Kundu, *Biotechnol. Adv.* **2010**, *28*, 325–347.
[12] F. Zheng, B. K. Cui, X. J. Wu, G. Meng, H. X. Liu, J. Si, *Int. Biodeterior. Biodegrad.* **2016**, *110*, 69–78.
[13] K. Labus, I. Gancarz, J. Bryjak, *Mater. Sci. Eng. C.* **2012**, *32*, 228–235.
[14] C. Chao, H. Guan, J. Zhang, Y. Liu, Y. Zhao, B. Zhang, *Water Sci. Technol.* **2018**, *77*, 809–818.
[15] E. Han, Y. Yang, Z. He, J. Cai, X. Zhang, X. Dong, *Anal. Biochem.* **2015**, *486*, 102–106.
[16] J. Kochana, K. Wapiennik, P. Knihnicki, A. Pollap, P. Janus, M. Oszajca, P. Kuśtrowski, *Anal. Bioanal. Chem.* **2016**, *408*, 5199–5210.
[17] Y. Li, L. Zhang, M. Li, Z. Pan, D. Li, *Chem. Cent. J.* **2012**, *6*, 1–8.
[18] W. Song, D. W. Li, Y. T. Li, Y. Li, Y. T. Long, *Biosens. Bioelectron.* **2011**, *26*, 3181–3186.
[19] J. R. Camargo, M. Baccarin, P. A. Raymundo-Pereira, A. M. Campos, G. G. Oliveira, O. Fatibello-Filho, O. N. Oliveira Jr, B. C. Janegitz, *Anal. Chim. Acta* **2018**, *1034*, 137–143.
[20] S. Chawla, R. Rawal, D. Kumar, C. S. Pundir, *Anal. Biochem.* **2012**, *430*,16–23.
[21] G. Zhou, J. Sun, M. Yaseen, H. Zhang, H. He, Y. Wang, H. Yang, J. Liang, M. Zhang, L. Zhou, *J. Electrochem. Soc.* **2018**, *165*, G11–G16.
[22] Z. Wang, Z. Dai, *Nanoscale* **2015**, *7*, 6420–6431.
[23] S. Chawla, R. Rawal, S. Sharma, C. S. Pundir, *Biochem. Eng. J.* **2012**, *68*, 76–84.
[24] J. Barkauskas, L. Mikoliunaite, I. Paklonskaite, P. Genys, J. J. Petroniene, I. Morkvenaite-Vilkonciene, A. Ramanaviciene, U. Samukaite-Bubniene, A. Ramanavicius, *Mater. Sci. Eng. C* **2019**, *98*, 515–523.
[25] E. Zor, Y. Oztekin, A. Ramanaviciene, Z. Anusevicius, H. Bingol, J. Barkauskas, M. Ersoz, A. Ramanavicius, *J. Electrochem. Soc.* **2014**, *161*, H3064–H3069.

[26] P. Sathishkumar, S. Kamala-Kannan, M. Cho, J. S. Kim, T. Hadibarata, M. R. Salim, B. T. Oh, *J. Mol. Catal. B* **2014**, *100*, 111–120.
[27] R. Xu, Q. Zhou, F. Li, B. Zhang, *Chem. Eng. J.* **2013**, *222*, 321–329.
[28] R. Xu, C. Chi, F. Li, B. Zhang, *ACS Appl. Mater. Interfaces* **2013**, *5*, 12554–12560.
[29] T. Palvannan, T. Saravanakumar, A. R. Unnithan, N. J. Chung, D. H. Kim, S. M. Park, *J. Mol. Catal. B* **2014**, *99*, 156–162.
[30] A. Pavinatto, L. A. Mercante, M. H. Facure, R. B. Pena, R. C. Sanfelice, L. H. Mattoso, D. S. Correa, *Appl. Surf. Sci.* **2018**, *458*, 431–437.
[31] E. I. Solomon, P. Chen, M. Metz, S. K. Lee, A. E. Palmer, *Angew. Chem. Int. Ed.* **2001**, *40*, 4570–4590.
[32] C. A. Ramsden, P. A. Riley, *Bioorg. Med. Chem.* **2014**, *22*, 2388–2395.
[33] T. Shams, R. J. Nasimudeen, S. Shazi, H. G. Nigel, A. Qamre, M. A. Adel, A. D. Ghazi, A. K. Mohammad, *CNS Neurol. Disord. Drug Targets* **2012**, *11*, 395–409.
[34] N. Durán, M. A. Rosa, A. D'Annibale, L. Gianfreda, *Enzyme Microb. Technol.* **2002**, *31*, 907–931.
[35] M. Scampicchio, A. Bulbarello, A. Arecchi, M. S. Cosio, S. Benedetti, S. Mannino, *Electroanalysis* **2012**, *24*, 719–725.
[36] L. S. Wan, B. B. Ke, Z. K. Xu, *Enzyme Microb. Technol.* **2008**, *42*, 332–339.
[37] S. Nataraj, K. Yang, T. Aminabhavi, *Prog. Polym. Sci.* **2012**, *32*, 487–513.
[38] R. M. Apetrei, N. Guven, P. Camurlu, *J. Electrochem. Soc.* **2022**, *169*, 020548.
[39] H. Hou, J. J. Ge, J. Zeng, Q. Li, D. H. Reneker, A. Greiner, S. Z. D. Cheng, *Chem. Mater.* **2005**, *17*, 967–973.
[40] S. Almuhamed, N. Khenoussi, L. Schacher, D. Adolphe, H. Balard, *J. Nanomater.* **2012**, *2012*, 750698.
[41] T. Kavetskyy, O. Smutok, O. Demkiv, I. Maťko, H. Švajdlenková, O. Šauša, I. Novák, D. Berek, K. Čechová, M. Pecz, *Mater. Sci. Eng. C* **2020**, *109*, 110570.
[42] Y. Wang, F. Zhai, Y. Hasebe, H. Jia, Z. Zhang, *Bioelectrochemistry* **2018**, *122*, 174–182.
[43] L. Silva, A. Salgado, M. Coelho, *Environ. Technol.* **2010**, *31*, 611–616.
[44] M. W. Ducey Jr, M. E. Meyerhoff, *Electroanalysis* **1998**, *10*, 157–162.
[45] K. Streffer, Doctoral Thesis, **2002**, Universität Potsdam.
[46] J. N. Rodriguez-Lopez, J. Tudela, R. Varon, F. Garcia-Carmona, F. Garcia-Canovas, *J. Biol. Chem.* **1992**, *267*, 3801–3810.
[47] Á. Sánchez-Ferrer, J. N. Rodríguez-López, F. García-Cánovas, F. García-Carmona, *Biochim. Biophys. Acta Protein Struct. Mol. Enzymol.* **1995**, *1247*, 1–11.
[48] B. Serra, S. Jiménez, M. Mena, A. Reviejo, J. Pingarrón, *Biosens. Bioelectron.* **2002**, *17*, 217–226.
[49] J. L. Muñoz-Muñoz, F. Garcia-Molina, P. A. García-Ruiz, M. Molina-Alarcon, J. Tudela, F. Garcia-Canovas, J. N. Rodriguez-Lopez, *Biochem. J.* **2008**, *416*, 431–440.
[50] E. Krol, J. L. Bolton, *Chem.-Biol. Interact.* **1997**, *104*, 11–27.
[51] K. Ikehata, J. A. Nicell, *Bioresour. Technol.* **2000**, *74*, 191–199.
[52] R. S. Brown, K. B. Male, J. H. Luong, *Anal. Biochem.* **1994**, *222*, 131–139.
[53] F. Campanhã Vicentini, L. L. C. Garcia, L. C. S. Figueiredo-Filho, B. C. Janegitz, O. Fatibello-Filho, *Enzyme Microb. Technol.* **2016**, *84*, 17–23.
[54] Y. Zou, D. Lou, K. Dou, L. He, Y. Dong, S. Wang, *J. Solid State Electrochem.* **2016**, *20*, 47–54.
[55] D. A. Oriero, I. O. Gyan, B. W. Bolshaw, I. F. Cheng, D. E. Aston, *Microchem. J.* **2015**, *118*, 166–175.
[56] F. M. Fartas, J. Abdullah, N. A. Yusof, Y. Sulaiman, M. I. Saiman, *Sensors* **2017**, *17*, 1132.
[57] J. Cabaj, A. Jędrychowska, A. Świst, J. Sołoducho, *Electroanalysis* **2016**, *28*, 1383–1390.
[58] İ. Polatoğlu, *J. Electrochem. Soc.* **2019**, *166*, B1620–B1629.
[59] F. A. A. Manan, W. W. Hong, J. Abdullah, N. A. Yusof, I. Ahmad, *Mater. Sci. Eng. C.* **2019**, *99*, 37–46.
[60] C. C. Mayorga-Martinez, M. Cadevall, M. Guix, J. Ros, A. Merkoçi, *Biosens. Bioelectron.* **2013**, *40*, 57–62.
[61] V. Carralero Sanz, M. L. Mena, A. González-Cortés, P. Yáñez-Sedeño, J. M. Pingarrón, *Anal. Chim. Acta* **2005**, *528*, 1–8.
[62] W. Rajesh, K. Takashima, Kaneto, *React. Funct. Polym.* **2004**, *59*, 163–169.
[63] M. Montereali, L. Della Seta, W. Vastarella, R. Pilloton, *J. Mol. Catal. B* **2010**, *64*, 189–194.
[64] R. S. Freire, N. Durán, L. T. Kubota, *J. Braz. Chem.* **2002**, *134*, 456–462.
[65] K. Streffer, E. Vijgenboom, A. W. Tepper, A. Makower, F. W. Scheller, G. W. Canters, U. Wollenberger, *Anal. Chim. Acta.* **2001**, *427*, 201–210.
[66] C. Nistor, J. Emnéus, L. Gorton, A. Ciucu, *Anal. Chim. Acta* **1999**, *387*, 309–326.
[67] H. B. Yildiz, J. Castillo, D. A. Guschin, L. Toppare, W. Schuhmann, *Microchim. Acta* **2007**, *159*, 27–34.
[68] H. M. Ali, A. M. El-Gizawy, R. E. I. El-Bassiouny, M. A. Saleh, *J. Food Sci. Technol.* **2015**, *52*, 3651–3659.
[69] J. Ros, J. Rodríguez-López, F. Garcia-Canovas, *Biochem. J.* **1993**, *295*, 309–312.
[70] A. Shrivastava, V. Gupta, *Chron. Young Sci.* **2011**, *2*, 21–25.
[71] N. Nesakumar, S. Sethuraman, U. M. Krishnan, J. B. B. Rayappan, *J. Comput. Theor. Nanosci.* **2014**, *11*, 2596–2602.

Manuscript received: March 10, 2022
Revised manuscript received: June 29, 2022
Accepted manuscript online: July 1, 2022
Version of record online: July 14, 2022